Available online at www.sciencedirect.com
SCIENCE DIRECT®
Ecological Modelling 180 (2004) 211–229
ECOLOGICAL MODELLING
www.elsevier.com/locate/ecolmodel

A forest growth and biomass module for a landscape simulation model, LANDIS: design, validation, and application

Robert M. Scheller*, David J. Mladenoff

Department of Forest Ecology and Management, University of Wisconsin-Madison, 1630 Linden Drive, Madison, WI 53706, USA

Received 23 June 2003; received in revised form 9 January 2004; accepted 9 January 2004

Abstract

Predicting the long-term dynamics of forest systems depends on understanding multiple processes that often operate at vastly different scales. Disturbance and seed dispersal are landscape-scale phenomena and are spatially linked across the landscape. Ecosystem processes (e.g., growth and decomposition) have high annual and inter-specific variation and are generally quantified at the scale of a forest stand. To link these widely scaled processes, we used biomass (living and dead) as an integrating variable that provides feedbacks between disturbance and ecosystem processes and feedbacks among multiple disturbances. We integrated a simple model of biomass growth, mortality, and decay into LANDIS, a spatially dynamic landscape simulation model. The new biomass module was statically linked to PnET-II, a generalized ecosystem process model. The combined model simulates disturbances (fire, wind, harvesting), dispersal, forest biomass growth and mortality, and inter- and intra-specific competition. We used the model to quantify how fire and windthrow alter forest succession, living biomass and dead biomass across an artificial landscape representative of northern Wisconsin, USA. In addition, model validation and a sensitivity analysis were conducted.

Keywords: Forest biomass; Aboveground net primary productivity; Fire regime; Wind throw; Succession; Shade tolerance; LANDIS; PnET-II

1. Introduction

The species composition, age structure, and landscape structure of forested landscapes results from the interaction of biological processes, abiotic constraints, and disturbances. These processes often operate at different scales and each process has unique temporal and spatial bounds. Ecosystem processes (e.g., net primary productivity, decomposition) have high variation at short temporal scales, e.g., from days to a year. Ecosystem process rates are dependent upon soils (Jenkins et al., 1999), climate (Aber et al., 1995), species composition (Aber and Federer, 1992; Ollinger et al., 1998), and succession (Sprugel, 1984; Gower et al., 1996; Binkley et al., 2002; Janisch and Harmon, 2002). Forest biomass, including both living and dead, is regulated by ecosystem processes, competition, and disturbance (Brown and Schroeder, 1999; Bugmann and Solomon, 2000). Biomass changes over years or decades when

* Corresponding author. Tel.: +1 608 265 6321.
E-mail address: rmscheller@wisc.edu (R.M. Scheller).

0304-3800/$ – see front matter © 2004 Elsevier B.V. All rights reserved.
doi:10.1016/j.ecolmodel.2004.01.022

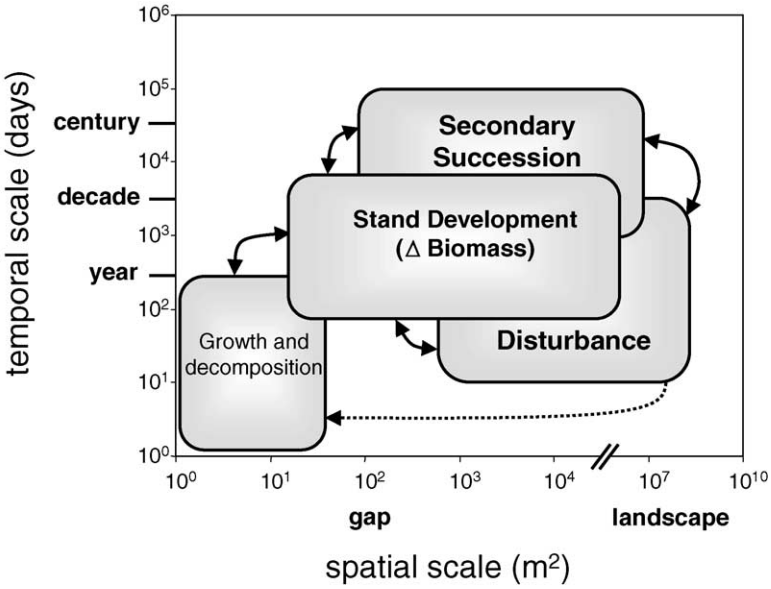

Fig. 1. Spatial and temporal scales at which different processes typically occur or are measured. Arrows represent direct interactions among processes.

undisturbed and is most often quantified at stand scales (Fig. 1). Forest biomass can affect ecosystem processes when high living biomass quantities favors regeneration by shade-tolerant, slower growing species (Abrams and Scott, 1989; Howard and Lee, 2002).

Aboveground biomass influences disturbance probability and severity (Romme, 1982; Miller and Urban, 1999; Canham et al., 2001). Disturbance events occur at spatial scales from small gaps (e.g., windthrow) to regions (e.g., drought) and are typically quantified at the temporal scale of years to decades. Disturbance selects against species with high disturbance susceptibility and can cause significant mortality of living biomass (Glitzenstein and Harcombe, 1988; Peterson and Pickett, 1995; Canham et al., 2001; Frelich, 2002; Scheller and Mladenoff, in press). In effect, biomass provides a record of previous disturbance events that integrates small-scale ecosystem processes and large-scale landscape processes. Analogous to an economic system, biomass can be seen as the 'currency' of a forested ecosystem.

A forested landscape is spatially dynamic and heterogeneous. Understanding forest dynamics requires a multi-scale approach that explicitly considers spatially dependent processes, such as disturbance. Accurate and meaningful predictions of forest dynamics require a conceptual understanding of the linkages among ecosystem processes, biomass stocks and accumulation rates, species composition, and spatially dependent processes. Our objectives were three-fold: (a) integrate ecosystem processes, aboveground living biomass, and dead biomass into a spatially interactive model of forest landscape change, (b) quantify the effect of multiple disturbances on aboveground biomass and species composition, and (c) evaluate model results and conduct a sensitivity analysis of the model parameters. The explicit question we used to demonstrate the model is: What are the effects of disturbance(s) on aboveground biomass, regeneration and succession in an artificial landscape representative of north central Wisconsin (USA)? Notwithstanding the initial domain of application, the model is broadly applicable for addressing questions about how multiple processes operating at disparate scales may influence forested landscapes.

2. Ecological background

How a disturbance affects biomass is highly dependent upon both the intensity and type of disturbance.

For all disturbances, we differentiate between *intensity*, the strength of a disturbance agent, and *severity*, a measure of the mortality caused by a disturbance. North central Wisconsin (USA) forests serve as our example and concomitant with this area, we focus on two natural disturbances: fire and wind.

A fire results from the combination of stochastic ignition events and the risk of burning and spreading. The fire regime, including fire size, frequency, and intensity, is a function of fuels (Romme, 1982; Miller and Urban, 1999), climate (Swetnam, 1993; Weisberg and Swanson, 2003), ignition frequency, management (Weisberg and Swanson, 2003), and landscape configuration (Bergeron and Brisson, 1990; Johnson, 1992; Turner and Romme, 1994). The effects of fire on biomass and regeneration vary significantly depending on fire frequency, fire intensity, and existing species. Locally, dead biomass may increase due to fire as mortality generally exceeds volatilization (Tinker and Knight, 2000). If fire is infrequent, regeneration opportunities for shade intolerant species are rare. However, infrequent, high intensity fires may provide regeneration opportunities for widely dispersed or serotinous species (He and Mladenoff, 1999b; Scheller and Mladenoff, in press). Very frequent fire may select for fire resistant species and decrease fire severity.

Wind disturbance is qualitatively different from fire and often creates significantly different landscape patterns. Blowdowns are more frequent and affect smaller individual areas than fire in northern Wisconsin (Zhang et al., 1999; Schulte and Mladenoff, in press). The location of wind events is stochastic, although wind severity varies as a function of the storm type. Wind severity (mortality) is a function of storm severity, species susceptibility (Webb, 1989), species size classes (Webb, 1989; Peterson, 2000; Canham et al., 2001), or, at the stand scale, total living biomass (Glitzenstein and Harcombe, 1988; Peterson, 2000; Canham et al., 2001). Topography can also influence wind severity (Boose et al., 1994; Foster et al., 1997).

On average, blowdowns leave more living biomass in place than do fires (Glitzenstein and Harcombe, 1988; Webb and Scanga, 2001; Peterson, 2000; Canham et al., 2001), providing fewer opportunities for early successional species. If storm severity is low, a wind disturbance may advance succession, dependent upon advanced regeneration (Abrams and Scott, 1989; Arevalo et al., 2000; Webb and Scanga, 2001). Intermediate intensity storms may benefit mid-successional species, such as *Betula alleghaniensis* (Peterson and Pickett, 1995; Canham et al., 2001). Only the most intense wind events (including tornados and hurricanes) significantly favor early successional species (Webb, 1989).

3. Model design

3.1. LANDIS: a forest landscape simulation model

We used a spatially explicit forest landscape model, LANDIS, to integrate ecosystem processes, biomass, and disturbance. LANDIS was designed to model large (10^4–10^6 ha) landscapes and simulate multiple disturbances (Mladenoff et al., 1996; He and Mladenoff, 1999b; Mladenoff and He, 1999). A LANDIS landscape is divided into many thousands of interacting, individual sites (or cells), of a size determined by the researcher. The sites are spatially linked together with fire, windthrow, seed dispersal, and other modules, including harvesting (Gustafson et al., 2000). Every site (or cell) belongs to a pre-defined ecoregion. An ecoregion is a user defined sub-region of the total landscape that is assumed to have homogeneous soil and climate attributes. Each ecoregion is assigned unique attributes, such as fire regime, wind regime, and the probability that a species can successfully become established. LANDIS currently operates on a ten-year time step.

LANDIS does not currently contain information that can be used to calculate aboveground living biomass, such as species or cohort diameters. Rather, individual tree species are represented as 10-year species-age cohorts, which are initiated when successful germination and establishment occurs. Nor does LANDIS natively track dead woody biomass quantities. We elected to preserve the existing cohort data structure, as it has been well validated and integrated with various disturbance modules, and add new state variables that supplement the existing data and allow aboveground living and dead woody biomass calculations. Based on our objectives and the computational limitations of complex landscape simulations, the biomass module was designed to minimize complexity. Biomass is calculated using a low number of parameters that can be estimated across an entire landscape.

3.2. Biomass module

The biomass module calculates ecosystem process rates and the quantity of aboveground living biomass (Mg ha^{-1}) for each tree species-age cohort. A single site often has >10 species-age cohorts, each of which has an associated living biomass value. Dead woody biomass (including all detritus and snags, excluding duff and litter) was amalgamated into a single value for each site. Biomass that is incorporated into the soil layer (soil organic carbon, SOC) was not modeled.

The biomass module interacts with all of the disturbance modules, allowing landscape processes to interact with each other through their effects on biomass (Fig. 2). All simulated mortality events (the death of a species-age cohort) either transferred the living biomass for a cohort to the dead biomass pool (in the case of fire or wind) or removed the living biomass from the system (in the case of harvesting). The biomass module will become an integral component of a new LANDIS version including new or modified disturbance modules (He et al., this volume; Yang et al., this volume; Shang et al., this volume) and more comprehensive feedbacks among biomass and various disturbances.

The biomass module calculates three processes rates: aboveground net primary productivity (ANPP), aboveground mortality (M), and woody biomass decomposition. Mortality is the rate of biomass transfer from the living biomass to the dead biomass pool. Mortality includes individual tree death, the loss of branches, and the annual loss of leaves or needles. On the basis of available ANPP data and models, the biomass module operates at an annual time step.

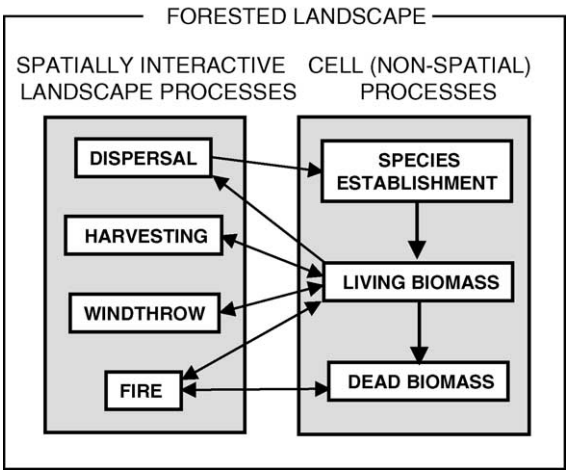

Fig. 2. Processes represented in LANDIS, including the biomass module.

3.2.1. Biomass module assumptions

A number of assumptions governed the development of the biomass module. The principle assumption was that an equilibrium condition would develop after many decades, whereas a cohort's mortality would equal growth, and biomass would cease to increase. Other components of the LANDIS model simulate changes in mortality due to disturbance. Without disturbance, the aboveground living biomass for each cohort (B_{ij}) at each time step is a function of the existing biomass, ANPP, and M (Acker et al., 2002):

$$B_{ij} = B_{ij} + \mathrm{ANPP}_{ij} - \mathrm{M}_{ij} \quad (1)$$

For all calculations, *i* represents a species present in a cell, *j* represents an age, *ij* is the species-age cohort. A summary of all variables is available in Table 1.

A second critical assumption was that, at the long time steps (10 years) modeled, disturbance does not significantly decrease maximum potential productivity by reducing available soil nitrogen. Based on a meta analysis of 39 studies, this assumption may be valid for wind and logging disturbance (Johnson and Curtis, 2001). The effect of fires on nitrogen are a function of fire severity; on average, fire increases soil nitrogen (Johnson and Curtis, 2001).

Long-term and landscape-scale data sets of growth and mortality were not readily available (e.g., Acker et al., 2000, 2002; Janisch and Harmon, 2002; Smithwick et al., 2002). Because LANDIS and the biomass module were designed to operate at broad scales, it was imperative that the biomass module was not reliant on data that are rarely available. Therefore, we calculated biomass growth and mortality using minimal representations based on logical assumptions and limited empirical data, where available. Our formulae for growth and mortality rates (Eqs. (4)–(6)) are based solely on our stated assumptions.

Lastly, we assumed that species-age cohort biomass data implicitly incorporates density information. Density was not explicitly calculated for either our growth or mortality functions. Density data may be essential

Table 1
Acronyms, definitions, and units for biomass model

Acronym	Definition	Units
$ANPP_{MAXi}$	Maximum ANPP for species *i*.	$Mg\,ha^{-1}\ year^{-1}$
$ANPP_{ACTij}$	Actual ANPP for species *i*, age cohort *j*.	$Mg\,ha^{-1}\,year^{-1}$
B_{ij}	Actual biomass—the amount of biomass for species *I*, age cohort *j*.	$Mg\,ha^{-1}$
B_{AMij}	The ratio of actual biomass to maximum biomass for species *i*, age cohort *j*.	NA
B_{MAXi}	Maximum possible biomass for species *i*.	$Mg\,ha^{-1}$
B_{POTij}	Potential biomass—the limit to the amount of biomass for species *i*, age cohort *j*, based on the 'growing space' available in a pixel. Must be less than B_{MAX}.	$Mg\,ha^{-1}$
B_{PMij}	The ratio of potential biomass to maximum biomass for species *i*, age cohort *j*.	NA
D_{ij}	Dead biomass, including both coarse woody debris (CWD) and snags.	$Mg\,ha^{-1}$
M_{BIOij}	Mortality rate as a function of total stand biomass.	$Mg\,ha^{-1}\,year^{-1}$
M_{AGEij}	Mortality rate as a function of species cohort age and maximum species longevity.	$Mg\,ha^{-1}\,year^{-1}$

for understanding the development of a single stand but is difficult or impossible to parameterize at the landscape scale. In particular, reductions in density over time are difficult to predict in mixed-species, mixed-age forests. Future research will explore variation in initial biomass as a function of seed rain and initial density.

3.2.2. Estimation of maximum ANPP for each species

First, we estimated maximum aboveground net primary productivity ($ANPP_{MAX}$) for each species, for each ecoregion (a region with homogeneous soil and climate attributes). $ANPP_{MAX}$ estimates for each species and ecoregion combination should be drawn from closed canopy forests, prior to the onset of any age-related decline in productivity (Sprugel, 1984; Gower et al., 1996; Ryan et al., 1997; Binkley et al., 2002), i.e., the maximum potential ANPP. Calculation of actual ANPP was performed separately and is discussed below. $ANPP_{MAX}$ was static, i.e., values remained constant for a species and ecoregion combination for the duration of the simulation.

A variety of data and technologies exist for estimating maximum potential productivity. $ANPP_{MAX}$ could be estimated from expert knowledge, Forest Inventory and Analysis (FIA) data (e.g., Brown et al., 1999; Brown and Schroeder, 1999; Jenkins et al., 2001), or empirically measured (e.g., Crow, 1978). Gap models (e.g., LINKAGES, Pastor and Post, 1986; ForClim, Bugmann and Solomon, 2000) and ecosystem process models (e.g., Biome-BGC, Running and Hunt, 1993; TEM, McGuire et al., 1992; Century, Parton et al., 1993) provide a generalized method for calculating $ANPP_{MAX}$.

3.2.3. Calculation of actual ANPP for each species-age cohort

Modeling aboveground living biomass for each species-age cohort required an estimation of actual ANPP ($ANPP_{ACT}$) at each time step. $ANPP_{ACT}$ was calculated independent of the time since disturbance. Time since disturbance is often used as a surrogate for canopy development when disturbance completely removes the canopy or living biomass data are not available. In reality, most disturbances do not completely remove the canopy and the amount of residual living biomass varies widely. Therefore, $ANPP_{ACT}$ was calculated as a function of the amount of living biomass existing at a site, irrespective of any prior disturbance that may have occurred.

We assumed that $ANPP_{ACT}$ increased logarithmically and asymptotically approached $ANPP_{MAX}$ as cohort biomass (B_{ij}) approached the maximum possible biomass for the cohort (B_{MAX}). Using Brown and Schroeder's (1999) data comparing ANPP and aboveground biomass, we estimated B_{MAXi} as a 30-fold increase over $ANPP_{MAX}$ for each species:

$$B_{MAXi}\,(Mg\,ha^{-1}) = ANPP_{MAXi}\,(Mg\,ha^{-1}) \times 30 \quad (2)$$

We also calculated a reduction of growth and mortality rate as a consequence of competition. If a stand contained more than one species-age cohort, the potential maximum biomass of each cohort was reduced. The potential biomass (B_{POTij}) represents the available 'growing space', minus space already occupied

by other species-age cohorts:

$$B_{\mathrm{POT}ij} = \min\left[0,\ B_{\mathrm{MAX}i} - \sum_{1}^{i}\sum_{1}^{j} B_{ij}\right] + B_{ij} \quad (3)$$

Current biomass (B_{ij}) was added to the growing space to exclude self-competition. A lower bounds (Eq. (3)) was necessary to ensure correct solutions for ANPP and mortality. Using these assumptions, we estimated $\mathrm{ANPP}_{\mathrm{ACT}ij}$ as:

$$\mathrm{ANPP}_{\mathrm{ACT}ij} = \mathrm{ANPP}_{\mathrm{MAX}i}(\mathrm{e}^{1} B_{\mathrm{AP}ij}\, \mathrm{e}^{-B_{\mathrm{AP}ij}}) B_{\mathrm{PM}ij} \quad (4)$$

where $B_{\mathrm{AP}ij}$ is the ratio of actual (B_{ij}) to potential (B_{POT}) biomass. Cohort productivity and mortality (see below) are both a function of $B_{\mathrm{AP}ij}$. A cohort with low biomass and large B_{POT} (i.e., a newly established cohort with low competition) would have low growth and mortality. When biomass is high relative to the available growing space, growth and mortality near equilibrium (Fig. 3a). $B_{\mathrm{PM}ij}$ is the ratio of potential biomass ($B_{\mathrm{POT}ij}$) to maximum biomass and limits productivity and mortality to accommodate multiple cohorts.

3.2.4. Calculation of mortality rates

Although other LANDIS algorithms calculate total cohort mortality, due to disturbance or age, it was also necessary to model partial cohort mortality, the mortality of individual trees or limbs within an age cohort. Such partial cohort mortality rates followed a different trajectory than ANPP. For each cohort, when living biomass was low, the mortality rate was also low (Acker et al., 2002). For simplicity, we assumed that cohort mortality did not exceed ANPP in the absence of disturbance or age-related mortality (below). Mortality increased logistically as biomass increased, until reaching equilibrium with ANPP. Mortality for a species-age cohort as a function of existing biomass was designated $\mathrm{M}_{\mathrm{BIO}ij}$. As with ANPP, mortality rates were calculated independent of the time since disturbance. A logistic equation was used to model $\mathrm{M}_{\mathrm{BIO}ij}$ (Fig. 3a):

$$\mathrm{M}_{\mathrm{BIO}ij} = \mathrm{ANPP}_{\mathrm{MAX}i}\left(\frac{y_0}{y_0 + (1-y_0)\mathrm{e}^{-r y_0^{-1} B_{\mathrm{AP}ij}}}\right) \times B_{\mathrm{PM}ij} \quad (5)$$

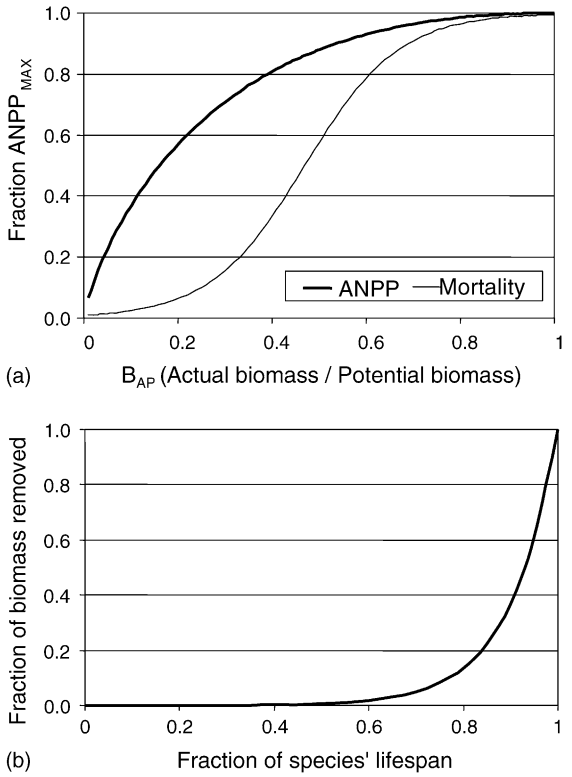

Fig. 3. (a) Correlation between aboveground net primary productivity ($\mathrm{ANPP}_{\mathrm{ACT}}$) and mortality ($\mathrm{M}_{\mathrm{BIO}}$) to the ratio of actual to potential biomass. (b) Age-related mortality ($\mathrm{M}_{\mathrm{AGE}}$) changing as a function of species lifespan.

where r is a growth parameter (default = 0.08) and y_0 is the initial decay rate rescaled from zero to one (default = 0.01).

In addition to mortality as a function of stand development (aboveground living biomass), we added age-related mortality as a species approached maximum longevity. Age-related mortality was modeled as an exponential increase in mortality with stand age:

$$\mathrm{M}_{\mathrm{AGE}ij} = B_{ij}\left(\frac{\mathrm{e}^{\mathrm{age}/\max \mathrm{age} \times d}}{\mathrm{e}^{d}}\right) \quad (6)$$

where d is a shape parameter (default = 10). If d = 10, age-related mortality would begin at one half of a species' lifespan, increase to ~14% of existing biomass at 80% lifespan, and reach 100% at 100% lifespan (Fig. 3b). Because $\mathrm{M}_{\mathrm{AGE}}$ was a fraction of B_{ij}, $\mathrm{M}_{\mathrm{AGE}}$ was subtracted from both $\mathrm{ANPP}_{\mathrm{ACT}}$ and $\mathrm{M}_{\mathrm{BIO}}$ to prevent the over-estimation of growth and mortality.

Total mortality equaled the sum of M_{BIO} and M_{AGE}. M_{AGE} simulated gap formation and therefore we allowed M_{AGE} to create additional growing space. Therefore, when $M_{AGE} > B_{POT}$, B_{POT} was set equal to M_{AGE}. This allowed young, shade tolerant cohorts with low biomass to continue growing slowly even when total site biomass was greater than B_{MAX}.

Annual mortality was divided into fine dead biomass (leaves) and dead woody biomass. Using dimensionless biomass production quotients from Niklas and Enquist (2002), annual leaf production ($ANPP_{leaf} = 0.35ANPP_{ACT}$) was subtracted from M_{BIO} annually. For age-related mortality, M_{AGE}, and disturbance caused mortality, we assumed that the fine dead biomass fraction was equal to $ANPP_{leaf} \times$ leaf longevity (Niklas and Enquist, 2002).

3.2.5. Calculation of decomposition

Decomposition of dead woody biomass (D) was modeled using an exponential decay equation:

$$D_{ij(t+1)} = D_{ij(t)}\, e^{-k} \quad (7)$$

where k was derived for each species (Tyrrell and Crow, 1994). The exponential decay model assumes that all constituents of dead biomass are equally decomposable and the constituents of dead woody biomass are equally distributed (Carpenter, 1981). As with maximum ANPP, values for k for each species in each ecoregion can be derived empirically (e.g., Harmon et al., 1986, 2000; Onega and Eickmeier, 1991; Tyrrell and Crow, 1994; Stone et al., 1998), estimated (e.g., Pastor and Post, 1986 [$k = 0.10$ for small wood, $k = 0.03$ for large wood]; Aber et al., 1991 [$k = 0.02$ for all wood]), or modeled (Burke et al., 2003). Values for k were static for each species-ecoregion combination, similar to $ANPP_{MAX}$ above. Decomposition of fine dead biomass was not initially modeled.

3.2.6. Calculation of shade

To calculate shade, we used a negative linear correlation between the natural log of percent full sunlight and the natural log of time (years) since complete disturbance (Howard and Lee, 2002). Howard and Lee (2002) quantified this correlation as a consequence of a 200-year stand development chronosequence in the northern hardwood forests of New Hampshire. Next, we assumed that the natural log of relative living biomass (the ratio of actual to maximum site biomass, B_{AM}, ranging from 0.1 to 1) increases linearly with the natural log of time, again over two hundred years. This correlation fit our simulations of aboveground living biomass over 200 years, beginning from ten percent maximum biomass, with an R^2 of 0.98. Using these two assumptions, we estimated the percentage of full sunlight as a function of relative biomass (B_{AM}) (Fig. 4a):

$$\text{Percent Full Sun} = e^{-2.85\, e^{B_{AM}} + 7.7513} \quad (8)$$

These calculations only apply when $B_{AM} > 0.10$. We assumed full sunlight was also 100% when $B_{AM} < 0.10$. Next, for each species where data were available, we plotted the minimum sunlight requirements for successful regeneration (Burns and Honkala, 1990) against our estimated shade tolerance values ($R^2 = 0.86$, Fig. 4b). Combining the two, we arrived at a maximum relative living biomass (B_{AM}) for each species shade tolerance class ($B_{AM} = 0.247, 0.326, 0.428, 0.588$ for shade classes 1–4, respectively). Species were not allowed to establish if B_{AM} exceeded the maximum B_{AM} for their shade tolerance class. It was assumed that

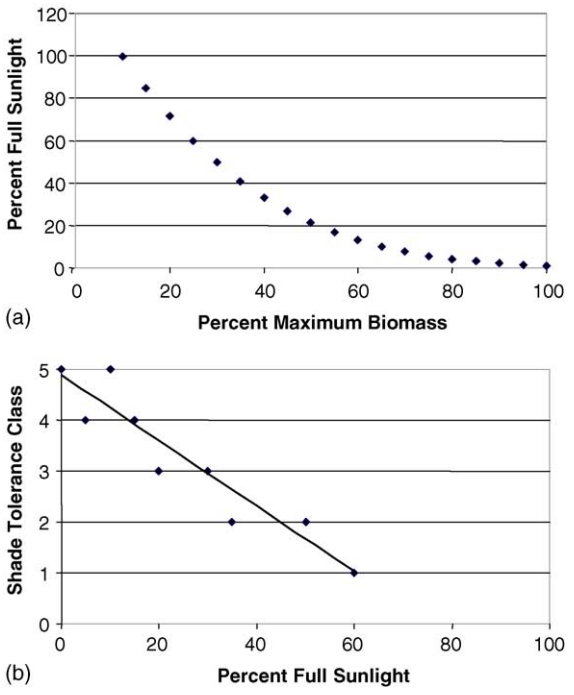

Fig. 4. (a) Percent full sunlight as a function of maximum biomass. (b) Minimum percent full sunlight required for species with varying shade tolerance classes.

shade tolerance class 5 species could establish under any amount of aboveground living biomass.

4. Experimental design and analysis

4.1. Test landscapes

Our goal for the test landscapes was to verify model behavior and qualitatively validate the interactions between the biomass module, disturbances, and the subsequent effects on shade and succession. The goal was not to simulate real landscape and disturbance dynamics. Therefore, we tested the model using a relatively small (<1000 ha) artificial landscape. Such a landscape allowed us to visualize and quantify the effects of individual disturbance events. Simulated disturbance sizes were also reduced, relative to historic sizes, so as to allow a range of rotation periods without requiring infrequent, catastrophic (>50% of the landscape disturbed) disturbances.

An artificial fractal landscape was generated with the RULE software (Gardner et al., 1987) for model testing and evaluation. A fractal landscape creates continuity of dead biomass, allowing fires to spread at the beginning of a model run. The test landscape contained a fractal arrangement of six communities containing 16 species typical of northern Wisconsin (Table 2) on a 99 × 99 grid (882 ha) with a cell size of 30 m. Six communities were created to represent potential forests for northern Wisconsin. All 16 species (Table 2) were included in at least one community.

At the beginning of a simulation, aboveground living and dead biomass values were initialized within LANDIS. The biomass module was iterated the number of time steps equal to the maximum cohort age for each site prior to beginning the model run. Each species-age cohort was grown the number of years equal to its initial cohort age. The biomass initialization included competition between cohorts. The initialization did not account for disturbances that may have happened prior to initialization and may overestimate initial live biomass and underestimate initial dead biomass quantities.

Scenarios of forest growth and change for a single site (a 900 m^2 cell) were also modeled to provide examples of model behavior at a fine scale. Three simple scenarios were chosen to demonstrate the general behavior of the model absent any disturbance and with or without competition: (a) a site initialized with a 10-year-old single cohort of a shade tolerant species (*Acer saccharum*); (b) a site initialized with a 10-year-old single cohort of a shade intolerant species (*Populus*

Table 2
Life history attributes, literature data for percent foliar nitrogen (%N) and leaf mass area (LMA), and maximum above ground net primary production for 16 species characteristic of northern Wisconsin

Species name	Longevity (years)	Shade tolerance	Fire tolerance	Mean %N	Maximum LMA ($g\,m^{-2}$)	Maximum ANPP ($Mg\,ha^{-1}\,year^{-1}$)
Abies balsamea	200	5	1	1.56 (6)	204 (6)	8.09
Acer rubrum	150	4	1	1.98 (2, 3, 4, 6)	75 (1, 2, 6)	7.46
Acer saccharum	400	5	1	2.13 (2, 4, 7)	85 (1, 2, 6, 7)	7.45
Betula alleghaniensis	350	4	2	2.34 (3, 6)	66 (6)	7.64
Betula papyrifera	120	2	2	2.22 (6)	100 (1, 6)	6.72
Fraxinus americana	300	4	1	2.03 (2, 3, 6)	76 (2, 6)	7.00
Picea glauca	300	3	2	1.34 (2, 7)	286 (2, 7)	6.50
Pinus banksiana	70	1	3	1.15 (2, 5)	244 (2, 7)	5.77
Pinus resinosa	250	2	4	1.25 (2, 3, 4, 7)	250 (2, 7)	5.01
Pinus strobus	450	3	3	1.71 (2, 3, 6, 7)	175 (2, 6, 7)	10.19
Populus tremuloides	120	1	2	2.33 (7)	83 (7)	7.46
Quercus ellipsoidalis	300	2	5	2.29 (2)	54 (2)	7.73
Quercus rubra	250	3	3	2.27 (2, 3, 4, 6)	105 (2, 6)	7.58
Thuja occidentalis	400	4	1	1.07 (2)	222 (2)	4.93
Tilia americana	250	4	2	2.71 (4, 6)	46 (6)	8.48
Tsuga canadensis	640	5	3	1.14 (3, 4, 6)	170 (6)	6.27

References: (1) Jurik (1986); (2) Reich et al. (1995); (3) Bolster et al. (1996); (4) Martin and Aber (1997); (5) Wallin and Raffa (1998); (6) Smith and Martin (2001); (7) Green et al. (2003).

tremuloides); and (c) a site initialized with two mature mid-tolerant species (*Pinus strobus* and *B. alleghaniensis*), and two young shade tolerant species (*A. saccharum* and *Tsuga canadensis*). Each of the three examples was limited to the initial species composition.

4.2. Scenarios and disturbance parameterization

Our questions and hypotheses were addressed using three wind scenarios and three fire scenarios for a total of nine scenarios. Each scenario ran for 300 years and was replicated four times for a total of 36 model runs. This allowed us to evaluate variability within each scenario due to stochastic fire and windthrow. Our response variables included fire and wind rotation periods, living biomass and dead biomass, and shade before and after a disturbance.

4.2.1. Wind disturbances

Three wind regimes were simulated, including a control (no wind). Wind event probabilities (WEP; 2×10^{-4}, 4×10^{-5}) were used to parameterize the wind scenarios. These are the probabilities of a windthrow being initiated at every site on the landscape at each model iteration. These probabilities would correspond to maximum wind rotation periods of 100 and 500 years, and were designated high and low, respectively. Because our modeled wind disturbances removed between 0 and 100% of the canopy, these values may be conservative (Frelich, 2002). Wind severity was modeled as a function of cohort age, species longevity (older cohorts are more vulnerable), and a randomly selected storm intensity. The location of a windthrow was randomly selected. Average windthrow size was parameterized at 44 ha (5% of the landscape) with a maximum of 88 ha (10%). Actual wind throw size was dependent upon the existence of susceptible cohorts.

4.2.2. Fire disturbances

Three fire regimes were simulated, including a control (no fire). We selected two ignition event probabilities (IEP, the probability of lightning or other sources of ignition occurring at every cell at each model iteration) to represent scenarios with frequent and moderate fire rotation periods. Because our goal was to examine disturbance interactions and effects on biomass, more historically accurate scenarios for mesic forests in northern Wisconsin (infrequent fire rotation periods >500 years) were not simulated. In LANDIS, the probability of actual fire ignition and spread is a function of time since last disturbance (a surrogate for fine fuels) or the presence of fine fuels generated by a wind event. The fuel accumulation curve (He and Mladenoff, 1999b) was held constant for all scenarios, with a maximum probability at 200 years. The ignition event probabilities were designated high (IEP for every active cell = 2×10^{-3}), and low (IEP = 1×10^{-4}). Average fire size was parameterized at 88 ha (10% of the landscape) with a maximum of 175 ha. Actual fire size was determined by the availability of fuels.

Fire intensity was modeled as a logarithmic function of dead woody biomass with maximum severity occurring immediately after a blowdown that destroyed >35% of the forest canopy. Cohort mortality was a function of fire intensity (He and Mladenoff, 1999a). For this initial model assessment, we assumed that dead woody biomass (including dead biomass from cohorts killed in the current fire) had a 24% burning efficiency for all fires, the maximum of previous estimates for temperate or boreal forests (20% in temperate forests, Seiler and Crutzen, 1980; 23% in Canadian boreal forests, French et al., 1994; 24% in Yellowstone National Park, Tinker and Knight, 2000).

4.3. Maximum ANPP parameterization

We parameterized $ANPP_{MAX}$ using PnET-II (Aber and Federer, 1992; Aber et al., 1995). PnET-II uses a simple approach to estimating $ANPP_{MAX}$ that is not dependent on initializations with SOC. Furthermore, PnET-II is initialized with species specific parameters, as is LANDIS. PnET-II was modified to use a relationship describing photosynthetic nitrogen use efficiency (PNUE) as a function of leaf mass per unit area (LMA, Green, 1998), replacing the correlation between foliar nitrogen and photosynthesis (Reich et al., 1995). PNUE was then multiplied by foliar nitrogen to determine photosynthetic capacity. Variation in LMA has been shown to exert a strong influence on the efficiency of nitrogen use in photosynthesis (Reich et al., 1997, 1998). The relationship between PNUE and LMA was used because it applies to both deciduous and conifer species and better captured interspecific variation (Fig. 5).

Input into PnET-II falls into three principle categories: ecoregion data, vegetation data, and climate data. Ecoregion data include mean latitude, growing

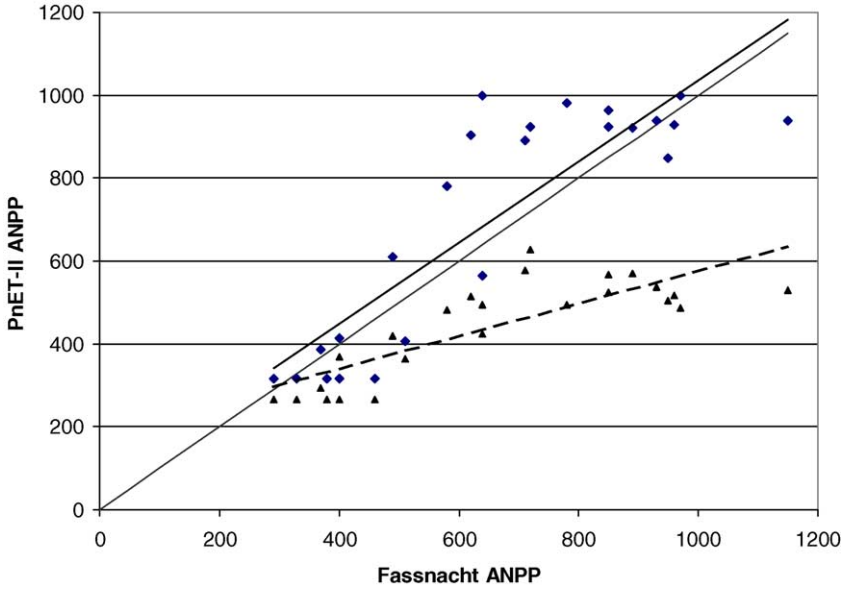

Fig. 5. Comparison of PnET-II estimated aboveground NPP and measured aboveground NPP data from Fassnacht (1996). Both the modified PnET-II (diamonds, thick solid line) and the original PnET-II (triangles, dashed line) were run with the same input data. 1:1 is shown as thin solid line. All units are $g\,m^{-2}$ $year^{-1}$.

degree days, and soil water holding capacity (WHC). Species parameters include foliar nitrogen, leaf mass area (LMA, $g\,m^{-2}$), carbon allocation, and others (Aber et al., 1995). Most of these variables have been defined previously (e.g., Aber et al., 1995; Reich et al., 1995). Values for mean foliar nitrogen (%) and maximum LMA for each species were compiled from literature for Wisconsin forests, if available, and other northern forests (Table 2). The maximum LMA was used because it was not always clear whether reported LMA values came from the top of the canopy, as required, or were a mean value for the entire canopy.

Monthly mean climatic variables (maximum temperature, minimum temperature, and precipitation) were calculated from a 30-year average from 1960 to 1990 (Zed, 1995) at 46°N latitude, 90°E longitude (approximate center of Vilas County, WI, USA). Soils were parameterized at 12 cm water holding capacity, a typical value for mesic soils in northern Wisconsin.

4.4. Model validation and sensitivity analysis

Model validation is a critical component of ecological modeling (Rykiel, 1996). However, validation of forest landscape models that operate at large spatial and temporal scales require different methods (Baker and Mladenoff, 1999). LANDIS is a stochastic model and does not produce predictions of actual events across the landscape. Furthermore, we did not simulate a real landscape. Consequently, traditional model validation against a known landscape is not possible.

Our validation goals were to validate PnET-II estimates of productivity and validate model estimates of biomass. Estimates for living or dead biomass were compared to published literature data. Validation of productivity estimates were conducted by comparing the performance of PnET-II against data from northern Wisconsin (Fassnacht, 1996; Fassnacht and Gower, 1997). The PnET-II validation was parameterized using species (weighted by basal area) and soil water holding capacity as recorded by Fassnacht (1996) and 1994 climatic data from the North Temperate Lakes Long-Term Ecological Research Station (Greenland and Kittel, 2002).

A sensitivity analysis of six key parameters was also performed: r (mortality rate growth parameter, Eq. (5), dimensionless); y_0 (initial mortality rate, rescaled to 0–1); d (age-related mortality shape parameter, Eq. (6), dimensionless); k (decomposition parameter, Eq. (7), dimensionless); the initial biomass of a new cohort

($0.5\,\mathrm{Mg\,ha^{-1}}$); and the ratio of $\mathrm{ANPP_{MAX}}$ to B_{MAX} (30, Eq. (2)). Values were varied by 10% and sensitivity was assessed for the landscape that most likely captured historic disturbance regimes (fire low, wind high). Parameters were varied by 10% ('confined to a small region around the standard parameter combination', Drechsler, 1998) in order to ensure that: (a) the state variable would linearly depend on the parameters and (b) as each parameter was varied, other model parameters would not also influence the state variable (Drechsler, 1998). Sensitivity was calculated as the percent change in mean biomass.

5. Results and discussion

5.1. ANPP validation

Our calculations of net primary productivity compared well to measured above ground NPP (Fig. 5, Fassnacht, 1996). The performance of PnET-II parameterized with literature data for species nitrogen and LMA, versus field collected data, suggests that the model could provide relatively accurate estimates of productivity across northern Wisconsin, similar to previous large-landscape applications (Aber et al., 1995; Ollinger et al., 1998; Jenkins et al., 1999). Applied to all 16 species and using the 30 year mean climatic data, PnET-II predicted an ANPP ranging from $4.93\,\mathrm{Mg\,ha^{-1}\,year^{-1}}$ (*Thuja occidentalis*) to $10.19\,\mathrm{Mg\,ha^{-1}\,year^{-1}}$ (*P. strobus*) (Table 2).

5.2. Single cell landscape examples

The first example, beginning with only a shade tolerant species, demonstrates model behavior with neither disturbance or inter-specific competition (Fig. 6a). Aboveground living biomass of *A. saccharum* reached an asymptote near $240\,\mathrm{Mg\,ha^{-1}}$. The woody mortality rate did not exceed the decomposition rate until year 50 and remained constant thereafter near $25\,\mathrm{Mg\,ha^{-1}}$. The second example, with only a shade intolerant species (Fig. 6b), demonstrates the effect of age limitation and shade intolerance. Aspen (*P. tremuloides*) biomass was cyclical with a maximum biomass ranging from 94 to $124\,\mathrm{Mg\,ha^{-1}}$. Decreases in living biomass were due to age-related mortality. Empirical measurements indicate that an aboveground live biomass range of

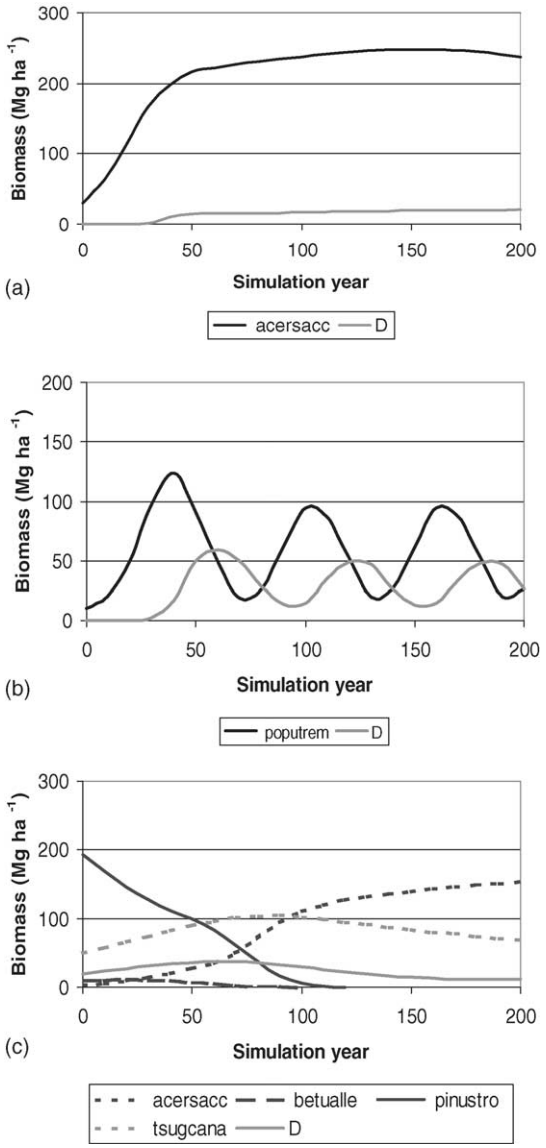

Fig. 6. Three examples of a single site changing over time. (a) Aboveground living biomass of *A. saccharum* (acersacc) and dead woody biomass (D). One species only. (b) Living biomass of *P. tremuloides* (poputrem) and dead biomass (D). One species only. (c) Living biomass of *P. strobus* (pinustro), *B. alleghaniensis* (betualle), *A. saccharum* (acersacc), *T. canadensis* (tsugcana), and dead biomass (D). All units are $\mathrm{Mg\,ha^{-1}}$.

95–$125\,\mathrm{Mg\,ha^{-1}}$ for mature aspen stands is typical (Table 3). Only after living biomass had declined to $19\,\mathrm{Mg\,ha^{-1}}$ was aspen able to regenerate and biomass began to increase again. The third example demon-

strates the effect of establishment priority and variable growth rates. Because of the existence of mature cohorts with large living biomass, the shade tolerant cohorts remained suppressed until the larger and older cohorts began to senesce (Fig. 6c). At year 90, *A. saccharum* surpassed *T. canadensis*, due to the higher maximum ANPP (Table 2).

5.3. Aboveground living and dead woody biomass validation

The aboveground living and dead woody biomass values produced by our model cannot be strictly validated due to our use of an artificial fractal landscape and artificial communities and the lack of detailed data for large landscapes without harvesting. Because FIA data, the only regional source of forest biomass data, were used to calibrate the model (Brown and Schroeder, 1999) and are heavily influenced by harvesting, these data could not be used for an unbiased validation. Nevertheless, available data suggest that model output is reasonably accurate. A simulated landscape with no fire had a living biomass of ~240 Mg ha^{-1} after the first 50 years (Fig. 7). This falls within the range of values for mature *A. saccharum* forest from the literature (Table 3), although greater than the 200 Mg ha^{-1} predicted as an upper bounds for second-growth forests in the Lake States (Crow, 1978). Maximum aboveground live biomass for the no disturbance scenario was 390 Mg ha^{-1}, near the estimate for old-growth *A. saccharum-T. canadensis* forests (Gries, 1995; Table 3). Modeled live biomass declined significantly as fire increased (Fig. 8a). Because natural fires were historically infrequent and fires are currently excluded or suppressed, these values are impossible to validate. However, where previous fires or harvesting has regenerated as aspen, our single site example (Fig. 6b) suggests that our model reasonably simulated the resultant live biomass. Overall, our model predictions of aboveground living biomass for northern Wisconsin were accurate, within the limits of the data available for validation.

Available literature data suggest a dead woody biomass range from 5 to 38 Mg ha^{-1} (Table 3). None of the literature data indicated recent catastrophic disturbance, although light disturbance or more distant disturbance events may not have been recorded. Our scenario without fire or wind equilibrated at a median dead woody biomass of 44.7 Mg ha^{-1} after 200 years. Our apparent overestimate may result from our inclusion of all dead woody debris, including snags, in the dead biomass pool and a single decay rate. However,

Table 3
Literature data for aboveground living biomass, dead biomass, age, and dominant species for mesic forests of Minnesota and Wisconsin

Source	Aboveground biomass (Mg ha^{-1})	Dead biomass (Mg ha^{-1})	Age (year)	Forest type
Gries (1995)	51	12.9	10	Acer-Tsuga
	225	5.3	40	Acer
	377	5.4	120	Acer-Tsuga
	398	23.3	>200	Acer-Tsuga
	291		>200	Acer
Crow (1978)	95			Populus
	96			Populus-Acer
	119			Acer-Betula
Mroz et al. (1985)	284		>200	Acer
	325		>200	Acer
Ruark and Bockheim (1988)	24	9.3	8	Populus
	40	10.5	14	Populus
	48	7.8	18	Populus
	102	13.0	32	Populus
	125	18.4	63	Populus
Harmon et al. (1986)		37.8	20	Acer-Betula
		16.0	40	Acer-Betula
		9.8	57	Acer-Fraxinus
		25.0	83	Acer-Betula

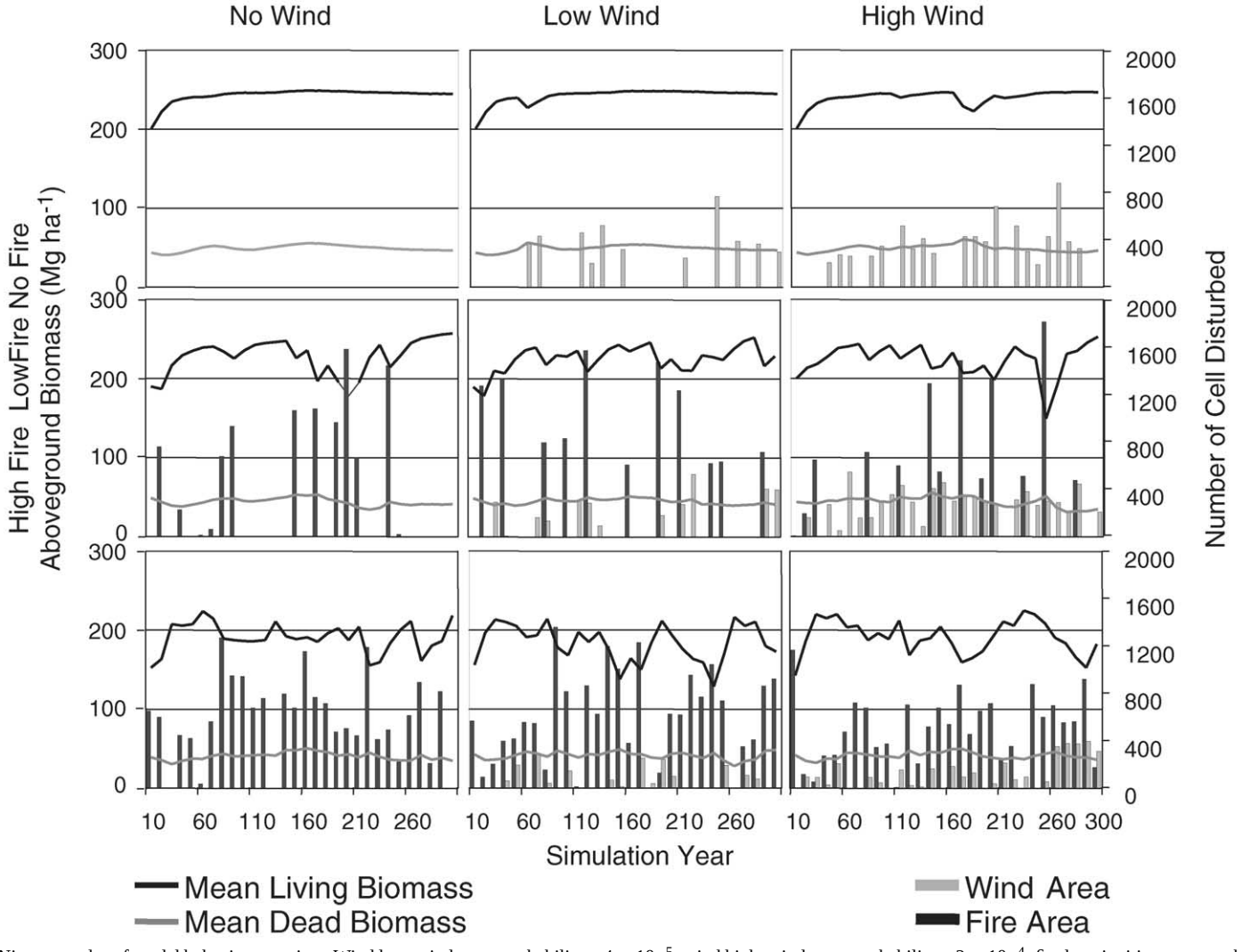

Fig. 7. Nine examples of model behavior over time. Wind low: wind event probability = 4×10^{-5}; wind high: wind event probability = 2×10^{-4}; fire low: ignition event probability = 1×10^{-4}; fire high: ignition event probability = 2×10^{-3}.

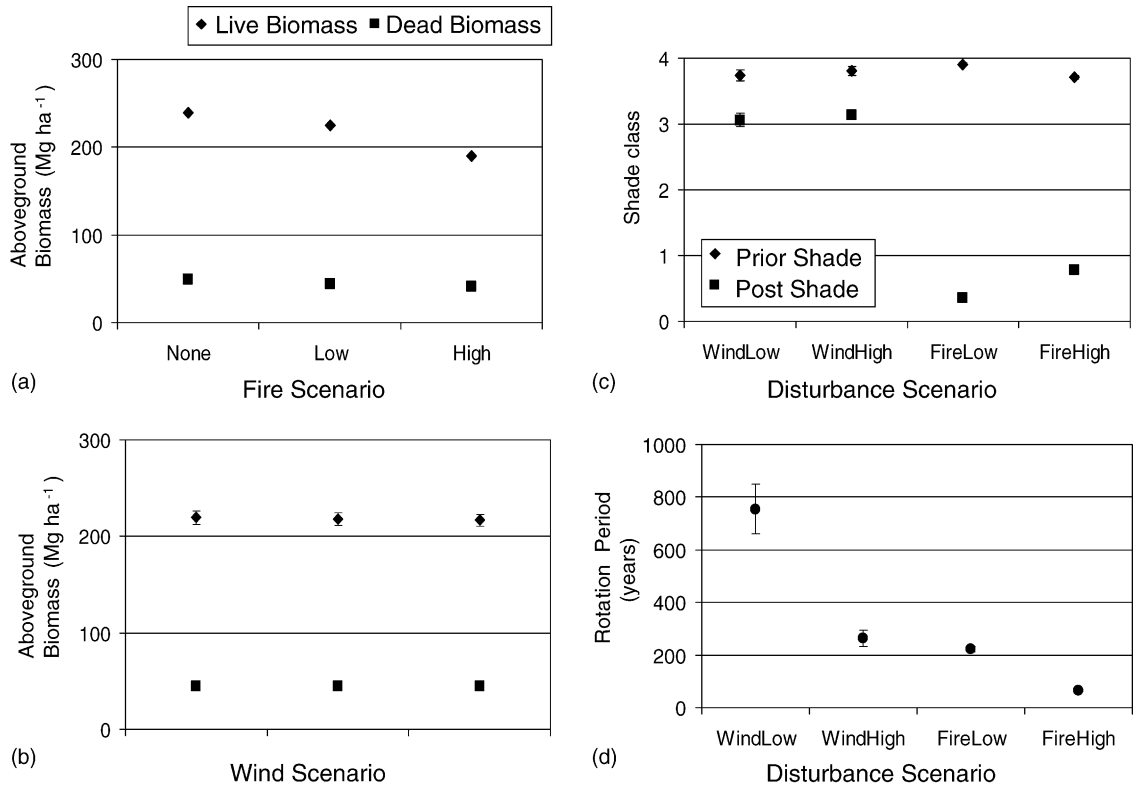

Fig. 8. Aboveground living and dead woody biomass as a function of (a) three fire scenarios and (b) three wind scenarios. (c) Pre- and post-disturbance shade as consequence of wind or fire disturbance scenarios. (d) Simulated wind and fire regimes. Error bars represent ±1 standard error ($N = 12$).

small diameter woody debris would be expected to decay faster than coarse dead biomass. Dead biomass did not differ significantly between fire or wind scenarios (Fig. 8a and b).

5.4. Sensitivity analysis

Our sensitivity analysis indicates that the biomass module is not sensitive to most of the parameters tested (Table 4). Living biomass deviation did not exceed 10%. Mean living biomass was most sensitive to a decrease in r, the mortality growth rate (Eq. (5)), and the ratio between maximum biomass (B_{MAX}) and maximum ANPP (Eq. (2)). The sensitivity to the maximum biomass-maximum ANPP ratio is not surprising, as this ratio defines the maximum possible living biomass for each cohort. Sensitivity to a decrease in r indicates that the living biomass model is moderately sensitive to the relationship between growth and mortality (Fig. 3a). Unfortunately, empirical data to better calibrate this relationship across a large landscape does not exist. Dead woody biomass was most sensitive to changes in the decomposition rate (k), with a 12.6% increase when k is decreased by 10% for every species (Table 4). Although the biomass model is generally robust to small parameter changes, the significance of parameter change is reduced overall by the highly stochastic nature of the total model. Also, parameter sensitivity may vary by disturbance scenario as each disturbance will emphasize different aspects of the biomass model. For example, dead biomass may demonstrate greater sensitivity if fire rotation periods increased. Likewise, living biomass may be sensitive to more or different parameters if the disturbance(s) simulated increased the number of rapidly growing cohorts.

Table 4
Sensitivity analysis for a scenario with frequent wind and infrequent fire

	Tested value	Percent change	Living biomass ($Mg\,ha^{-1}$)	Standard error	Percent change	Dead biomass ($Mg\,ha^{-1}$)	Standard error	Percent change
Original			178.8	0.9		35.3	0.5	
r	0.088	10	175.3	2.6	−1.99	35.3	0.3	−0.14
	0.072	−10	187.3	2.5	4.73	35.3	0.5	−0.14
y_0	0.011	10	184.8	3.4	3.33	34.5	0.3	−2.27
	0.009	−10	172.3	3.0	−3.66	37.0	0.4	4.82
d	11	10	176.3	2.2	−1.43	35.5	0.6	0.57
	9	−10	174.8	1.6	−2.27	36.5	0.3	3.40
k (by species)		10	179.0	1.3	0.11	31.3	0.5	−11.47
		−10	177.3	1.5	−0.87	39.8	0.3	12.61
Initial biomass	550	10	174.8	3.4	−2.27	35.5	1.0	0.57
	450	−10	179.3	5.0	0.25	35.8	1.1	1.27
B_{MAX}:$ANPP_{MAX}$	27	10	162.5	1.0	−9.12	35.8	0.3	1.27
	33	−10	194.5	0.5	8.78	35.0	0.6	−0.85

r: mortality rate parameter (parameter); y_0: initial mortality rate, rescaled to 0–1; d: age-related mortality shape parameter (dimensionless); k: decomposition parameter (dimensionless); initial biomass: initial biomass of a new cohort ($0.5\,Mg\,ha^{-1}$); (B_{MAX}:$ANPP_{MAX}$): the ratio of B_{MAX} to $ANPP_{MAX}$.

5.5. Fire, wind, and shade interactions

The simulated fire regimes affected both aboveground living biomass and shade and provided more opportunities for shade tolerance classes to become established (Fig. 8a and c). Frequent fires caused less shade reduction than infrequent fires (Fig. 8c), possibly due to increased dominance of fire tolerant species. Therefore, fire severity (living biomass mortality) was affected by fire frequency, similar to model results from northern Minnesota (Scheller and Mladenoff, in press).

Wind did not significantly alter living biomass (Fig. 8b) and had a relatively minor effect on shade (Fig. 8c). The broad range of wind severities simulated, with a minimum of <10% biomass mortality and relatively small average size (33 ha), may have precluded significant effects at the landscape scale. Other research has also found minor effects on structure or community following windstorms in Minnesota (Webb and Scanga, 2001) and Pennsylvania (Peterson, 2000), although these studies measured forest change after known wind events. We did not find evidence that wind accelerated succession (e.g., Abrams and Scott, 1989; Arevalo et al., 2000; Webb and Scanga, 2001), although we did not separate wind effects by storm intensity in our analysis. Light wind events may have accelerated succession for individual blow downs. Overall, our results suggest that species typical of mesic forests are at greater mortality risk due to a fire event than a wind event. Wind and fire may interact and influence the frequency and size of each other. These interactions, and interactions with harvesting, will be explored in future research.

The effect of disturbance on shade was significantly different between wind and fire events (Fig. 8c). Both disturbance types began in stands with relatively high shade values. Wind events reduced shade by less than one shade category, on average, with no difference between the infrequent and frequent wind scenarios (Fig. 8c). Fire reduced shade by greater than two shade categories; infrequent fire regimes reduced shade more. The ability of wind and fire to reduce shade and create regeneration opportunities for species with varying shade tolerance was assessed by plotting changing dominance over time. Five dominance classes corresponding to each shade tolerance class were plotted over time for each scenario; dominance is determined by total living biomass for each class (Table 2; Fig. 9).

As wind frequency increased (from zero to high wind) without fire or with light fire, the ability of shade tolerance class 4 (shade tolerance class 5 is the most shade tolerant) to persist increased. Empirical data have demonstrated that intermediate intensity storms can benefit mid-successional species (Peterson and Pickett,

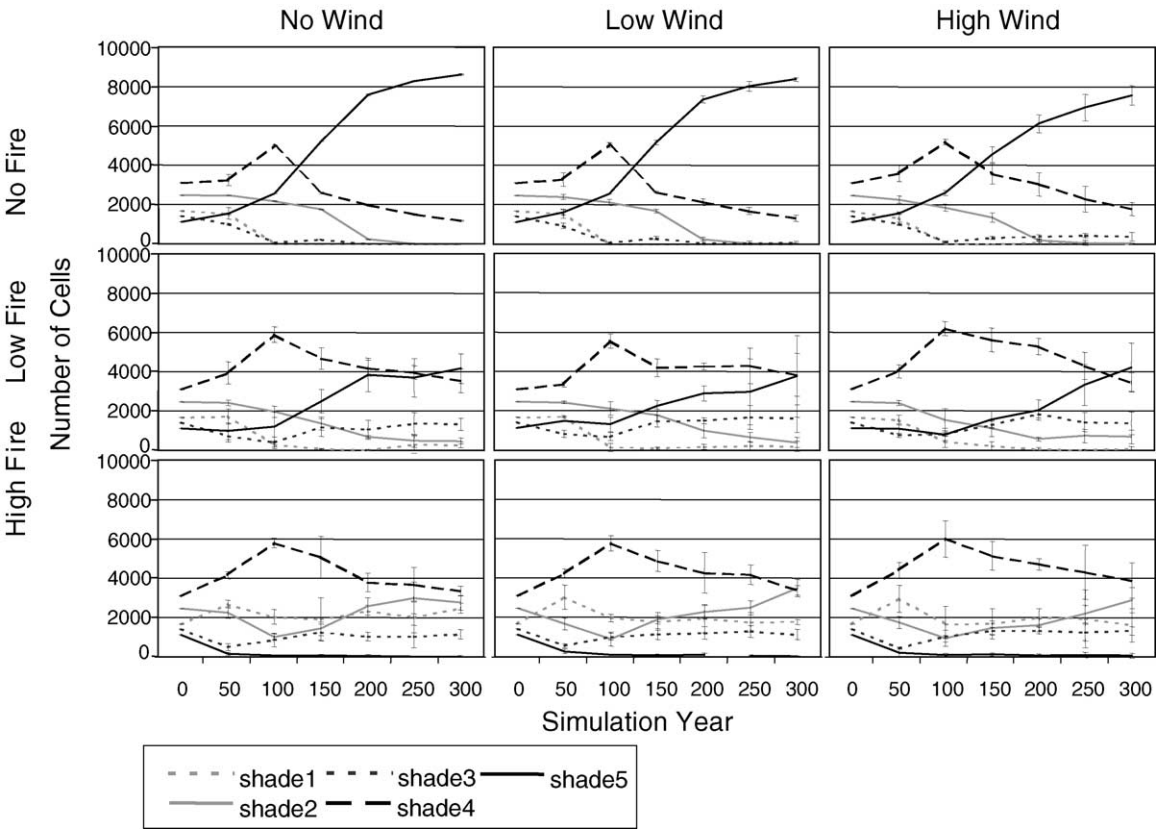

Fig. 9. Forest landscape dominance of five shade tolerance classes during a 300-year simulation with three fire scenarios and three wind scenarios. Error bars represent ±1 standard error ($N = 4$).

1995; Canham et al., 2001). With a light fire regime and increasing wind frequency, shade class 5 was reduced and all other shade classes increased. Wind had a minor effect when fire ignition frequency was high (Fig. 9). As fire frequency increased, shade class 5 dominance invariably decreased with a subsequent increase in shade classes 1–4. Shade class 1 (very shade intolerant), declined over time even when fires were frequent, reflecting an increase in fire tolerant species. The wind regime delayed the emergence of some shade classes. When fire was low, shade class 5 dominance was delayed as wind frequency increased. Likewise, when fire was high, shade class 2 dominance was delayed.

6. Conclusions

Our model provided aboveground living and dead woody biomass estimates using a non-mechanistic, semi-empirical representation of ecosystem processes that requires minimal parameterization. The original LANDIS model was written to facilitate research on disturbances occurring over large spatial and long temporal scales. Our biomass module, described herein, functions at the same conceptual scale and utilizes the same functional units (species-age cohorts), while providing additional quantitative information. Estimating the quantitative effects of disturbance(s), dispersal, and ecosystem processes on forest biomass will be imperative as we move forward into an era where many ecosystem process rates may begin changing at unprecedented rates.

Using our new model, we were able to simulate the interactions between wind, fire, shade, and succession. The results increase our understanding of the respective roles that fire and wind have in determining forest landscape dynamics. Furthermore, our results validate our representation of a critical process: succession as a

consequence of individual species' shade tolerance. As the validation of landscape model predictions remains difficult at best, the validation of component process representation is paramount.

Our model provides an important feedback between ecosystem processes (e.g., growth and decay rates) and landscape processes that operate at larger spatial and temporal scales. The success of future disturbance simulations, particularly climate change, on forested landscapes will be dependent on a better understanding of the link between ecosystem processes and the larger landscape. The model provides opportunities for evaluating the interactions among many different disturbance types and the feedbacks among disturbances and biomass.

Acknowledgements

Thanks to Barry DeZonia for generous programming support and the Forest Landscape Ecology Laboratory for additional support. Dr. Eric L. Kruger provided substantial assistance with PnET-II parameterization and recoding. Dr. Eric Gustafson and Dr. Brian Sturtevant both provided invaluable help through their guidance of the LANDIS development team and additional assistance with this manuscript. The research was funded by the U.S. Forest Service North Central Research Station and the National Fire Plan. Dr. Volker Radeloff, Dr. M.L. Smith, dissertation committee members of R.M. Scheller, and one anonymous reviewer provided important guidance and feedback.

References

Aber, J.D., Federer, C.A., 1992. A generalized, lumped-parameter model of photosynthesis, evapotranspiration and net primary production in temperate and boreal forest ecosystems. Oecologia 92, 463–474.

Aber, J.D., Melillo, J.M., Nadelhoffer, K.J., Pastor, J., Boone, R.D., 1991. Factors controlling nitrogen cycling and nitrogen saturation in northern temperate forest ecosystems. Ecol. Appl. 1, 303–315.

Aber, J.D., Ollinger, S.V., Federer, C.A., Reich, P.B., Goulden, M.L., Kicklighter, D.W., Melillo, J.M., Lathrop Jr., R.G., 1995. Predicting the effects of climate change on water yield and forest production in the northeastern United States. Climate Res. 5, 207–222.

Abrams, M.D., Scott, M.L., 1989. Disturbance-mediated accelerated succession in two Michigan forest types. For. Sci. 35, 42–49.

Acker, S.A., Halpern, C.B., Harmon, M.E., Dyrness, C.T., 2002. Trends in bole biomass accumulation, net primary production and tree mortality in *Pseudotsuga menziesii* forests of contrasting age. Tree Physiol. 22, 213–217.

Acker, S.A., Harcombe, P.A., Harmon, M.E., Green, S.E., 2000. Biomass accumulation over the first 150 years in coastal Oregon *Picea-Tsuga* forest. J. Veg. Sci. 11, 725–738.

Arevalo, J.R., DeCoster, J.K., McAlister, S.D., Palmer, M.W., 2000. Changes in two Minnesota forests during 14 years following catastrophic windthrow. J. Veg. Sci. 11, 833–840.

Baker, W.L., Mladenoff, D.J., 1999. Progress and future directions in spatial modeling of forest landscapes. In: Mladenoff, D.J., Baker, W.L. (Eds.), Spatial Modeling of Forest Landscape Change. Cambridge University Press, Cambridge, UK, pp. 333–349.

Bergeron, Y., Brisson, J., 1990. Fire regime in red pine stand at the northern limit of the species' range. Ecology. 71, 1352–1364.

Binkley, D., Stape, J.L., Ryan, M.G., Barnard, H.R., Fownes, J., 2002. Age-related decline in forest ecosystem growth: an individual-tree, stand-structure hypothesis. Ecosystems 5, 58–67.

Bolster, K.L., Martin, M.E., Aber, J.D., 1996. Determination of carbon fraction and nitrogen concentration in tree foliage by near infrared reflectance: a comparison of statistical methods. Can. J. For. Res. 26, 590–600.

Boose, E.R., Foster, D.R., Fluet, M., 1994. Hurricane impacts to tropical and temperate forest landscapes. Ecol. Monogr. 64, 369–400.

Brown, S.L., Schroeder, P., Kern, J.S., 1999. Spatial distribution of biomass in forests of the eastern USA. For. Ecol. Manage. 123, 81–90.

Brown, S.L., Schroeder, P.E., 1999. Spatial patterns of aboveground production and mortality of woody biomass for eastern U.S. forests. Ecol. Appl. 9, 968–980.

Bugmann, H.K.M., Solomon, A.M., 2000. Explaining forest composition and biomass across multiple biogeographical regions. Ecol. Appl. 10, 95–114.

Burke, I.C., Kaye, J.P., Bird, S.P., Hall, S.A., McCulley, R.L., Sommerville, G.L., 2003. Evaluating and testing models of terrestrial biogeochemistry: the role of temperature in controlling decomposition. In: Canham, C.D., Cole, J.J., Lauenroth, W.K. (Eds.), The Role of Models in Ecosystem Science. Princeton University Press, Princeton, New Jersey, USA, pp. 225–253.

Burns, R.M., Honkala, B.H. (Technical coordinators), 1990. Silvics of North America: 1. Conifers; 2. Hardwoods. Agriculture Handbook, vol. 654. U.S. Department of Agriculture, Forest Service, Washington, DC, USA.

Canham, C.D., Papaik, M.J., Latty, E.F., 2001. Interspecific variation in susceptibility to windthrow as a function of tree size and storm severity for northern temperate tree species. Can. J. For. Res. 31, 1–10.

Carpenter, S.R., 1981. Decay of heterogeneous detritus: a general model. J. Theor. Biol. 89, 539–547.

Crow, T.R., 1978. Biomass and production in three contiguous forests in northern Wisconsin. Ecology 59, 265–273.

Drechsler, M., 1998. Sensitivity analysis of complex models. Biol. Conserv. 86, 401–412.

Fassnacht, K.S., 1996. Characterization of the structure and function of upland forest ecosystems in North Central Wisconsin. Dissertation, University of Wisconsin-Madison, Madison, WI, USA.

Fassnacht, K.S., Gower, S.T., 1997. Interrelationships among the edaphic and stand characteristics, leaf area index, and aboveground productivity of upland forest ecosystems in north central Wisconsin. Can. J. For. Res. 27, 1058–1067.

Foster, D.R., Aber, J.D., Melillo, J.M., Bowden, R.D., Bazzaz, F.A., 1997. Forest response to disturbance and anthropogenic stress. Bioscience 47, 437–445.

Frelich, L.E., 2002. Forest Dynamics and Disturbance Regimes: Studies from Temperate Evergreen-Deciduous Forests. Cambridge University Press, Cambridge, UK.

French, N.H.F., Kasischke, E.S., Stocks, B.J., Mudd, J.P., Martell, D.L., Lee, B.S., 1994. Carbon release from fires in the North American boreal forest. In: Kasischke, E.S., Stocks, B.J. (Eds.), Fire, Climate, and Carbon Cycling in the Boreal Forest. Springer-Verlag, New York, NY, USA, pp. 377–388.

Gardner, R.H., Milne, B.T., Turner, M.G., O'Neill, R.V., 1987. Neutral models for the analysis of broad-scale landscape pattern. Landscape Ecol. 1, 19–28.

Glitzenstein, J.S., Harcombe, P.A., 1988. Effects of the December 1983 tornado on forest vegetation of the Big Thicket, southeast Texas, USA. For. Ecol. Manage. 25, 269–290.

Gower, S.T., McMurtrie, R.E., Murty, D., 1996. Aboveground net primary production decline with stand age: potential causes. Trends Ecol. Evol. 11, 378–382.

Green, D.S., 1998. Interrelation of leaf structure and function among deciduous broad-leaved and evergreen needle-leaved trees in Southern Wisconsin. Dissertation, University of Wisconsin-Madison, Madison, WI, USA.

Green, D.S., Erickson, J.E., Kruger, E.L., 2003. Foliar morphology and canopy nitrogen as predictors of light-use efficiency in terrestrial vegetation. Agric. For. Meteorol. 115, 165–173.

Greenland, D., Kittel, T.G.F., 2002. Temporal variability of climate at the US long-term ecological research (LTER) sites. Climate Res. 19, 213–231.

Gries, J.F., 1995. Biomass and net primary production for a Northern Hardwood Stand developmental sequence in the Upper Peninsula, Michigan. Thesis, University of Wisconsin-Madison, Madison, WI, USA.

Gustafson, E.J., Shifley, S.R., Mladenoff, D.J., Nimerfro, K.K., He, H.S., 2000. Spatial simulation of forest succession and timber harvesting using LANDIS. Can. J. For. Res. 30, 32–43.

Harmon, M.E., Franklin, J.F., Swanson, F.J., Sollins, P., Gregory, S.V., Lattin, J.D., Anderson, N.H., Cline, S.P., Aumen, N.G., Sedell, J.R., Lienkaemper, G.W., Cromack Jr., K., Cummins, K.W., 1986. Ecology of coarse woody debris in temperate ecosystems. Adv. Ecol. Res. 15, 133–302.

Harmon, M.E., Krankina, O.N., Sexton, J., 2000. Decomposition vectors: a new approach to estimating woody detritus decomposition dynamics. Can. J. For. Res. 30, 76–84.

He, H.S., Mladenoff, D.J., 1999a. The effects of seed dispersal on the simulation of long-term forest landscape change. Ecosystems 2, 308–319.

He, H.S., Mladenoff, D.J., 1999b. Spatially explicit and stochastic simulation of forest landscape fire disturbance and succession. Ecology 80, 81–99.

Howard, L.F., Lee, T.D., 2002. Upland old-field succession in southeastern New Hampshire. J. Torrey Bot. Soc. 129, 60–76.

Janisch, J.E., Harmon, M.E., 2002. Successional changes in live and dead wood carbon stores: implications for net ecosystem productivity. Tree Physiol. 22, 77–89.

Jenkins, J.C., Birdsey, R.A., Pan, Y., 2001. Biomass and NPP estimation for the mid-Atlantic region (USA) using plot-level forest inventory data. Ecol. Appl. 11, 1174–1193.

Jenkins, J.C., Kicklighter, D.W., Ollinger, S.V., Aber, J.D., Melillo, J.M., 1999. Sources of variability in net primary production predictions at a regional scale: a comparison using PnET-II and TEM 4.0 in northeastern US forests. Ecosystems 2, 555–570.

Johnson, D.W., Curtis, P.S., 2001. Effects of forest management on soil C and N storage: meta analysis. For. Ecol. Manage. 140, 227–238.

Johnson, E.A., 1992. Fire and Vegetation Dynamics: Studies from the North American Boreal Forest. Cambridge University Press, Cambridge, UK (129 pp.).

Jurik, T.W., 1986. Temporal and spatial patterns of specific leaf weight in successional northern hardwood tree species. Am. J. Bot. 73, 1083–1092.

Martin, M.E., Aber, J.D., 1997. High spectral resolution remote sensing of forest canopy lignin, nitrogen, and ecosystem processes. Ecol. Appl. 7, 431–443.

McGuire, A.D., Melillo, J.M., Joyce, L.A., Kicklighter, D.W., Grace, A.L., Moore III, B., Vorosmarty, C.J., 1992. Interactions between carbon and nitrogen dynamics in estimating net primary productivity for potential vegetation in North America. Global Biogeochem. Cycles 6, 101–124.

Miller, C., Urban, D.L., 1999. Forest pattern, fire, and climatic change in the Sierra Nevada. Ecosystems 2, 76–87.

Mladenoff, D.J., He, H.S., 1999. Design, behavior and application of LANDIS, an object-oriented model of forest landscape disturbance and succession. In: Mladenoff, D.J., Baker, W.L. (Eds.), Spatial Modeling of Forest Landscape Change. Cambridge University Press, Cambridge, UK, pp. 125–162.

Mladenoff, D.J., Host, G.E., Boeder, J., Crow, T.R., 1996. LANDIS: a spatial model of forest landscape disturbance, succession, and management. In: Goodchild, M.F., Steyaert, L.T., Parks, B.O., Johnston, C., Maidment, D., Crane, M., Glendinning, S. (Eds.), GIS and Environmental Modeling: Progress and Research Issues. GIS World Books, Fort Collins, CO, USA, pp. 175–179.

Mroz, G.D., Gale, M.R., Jurgensen, M.F., Frederick, D.J., Clark III, A., 1985. Composition, structure, and aboveground biomass of two old-growth northern hardwood stands in Upper Michigan. Can. J. For. Res. 15, 78–82.

Niklas, K.J., Enquist, B.J., 2002. Canonical rules for plant organ biomass partitioning and annual allocation. Am. J. Bot. 89, 812–819.

Ollinger, S.V., Aber, J.D., Federer, C.A., 1998. Estimating regional forest productivity and water yield using an ecosystem model linked to a GIS. Landscape Ecol. 13, 323–334.

Onega, T.L., Eickmeier, W.G., 1991. Woody detritus inputs and decomposition kinetics in a southern temperate deciduous forest. Bull. Torrey Bot. Club. 118, 52–57.

Parton, W.J., Scurlock, J.M.O., Ojima, D.S., Gilmanov, T.G., Scholes, R.J., Schimel, D.S., Kirchner, T., Menaut, J.C., Seastedt, T., Garcia Moya, E., Kamnalrut, A., Kinyamario, J.I., 1993. Observations and modeling of biomass and soil organic matter dynamics for the grassland biome worldwide. Global Biogeochem. Cycles 7, 785–809.

Pastor, J., Post, W.M., 1986. ORNL/TM-9519. Oak Ridge National Laboratory, Oak Ridge, TN, USA.

Peterson, C.J., 2000. Damage and recovery of tree species after two different tornadoes in the same old growth forest: a comparison of infrequent wind disturbances. For. Ecol. Manage. 135, 237–252.

Peterson, C.J., Pickett, S.T.A., 1995. Forest reorganization: a case study in an old-growth forest catastrophic blowdown. Ecology 76, 763–774.

Reich, P.B., Ellsworth, D.S., Walters, M.B., 1998. Leaf structure (specific leaf area) modulates photosynthesis-nitrogen relations: evidence from within and across species and functional groups. Funct. Ecol. 12, 948–958.

Reich, P.B., Kloeppel, B.D., Ellsworth, D.S., Walters, M.B., 1995. Different photosynthesis-nitrogen relations in deciduous hardwood and evergreen coniferous tree species. Oecologia 104, 24–30.

Reich, P.B., Walters, M.B., Ellsworth, D.S., 1997. From tropics to tundra: global convergence in plant functioning. Proc. Natl. Acad. Sci. U.S.A. 94, 13730–13734.

Romme, W.H., 1982. Fire and landscape diversity in subalpine forests of Yellowstone National Park. Ecol. Monogr. 52, 199–221.

Ruark, G.A., Bockheim, J.G., 1988. Biomass, net primary production, and nutrient distribution for an age sequence of *Populus tremuloides* ecosystems. Can. J. For. Res. 18, 435–443.

Running, S.W., Hunt Jr., E.R., 1993. Generalization of a forest ecosystem process model for other biomes, BIOME-BGC and an application for global scale models. In: Ehleringer, J.R., Field, C.B. (Eds.), Scaling Physiological Processes: Leaf to Globe. Academic Press Inc., San Diego, CA, USA, pp. 141–158.

Ryan, M.G., Binkley, D., Fownes, J.H., 1997. Age-related decline in forest productivity: pattern and process. Adv. Ecol. Res. 27, 213–262.

Rykiel Jr., E.J., 1996. Testing ecological models: the meaning of validation. Ecol. Model. 90, 229–244.

Scheller, R.M., Mladenoff, D.J., in press. Simulating the effects of fire reintroduction versus continued suppression on forest composition and landscape structure in the Boundary Waters Canoe Area, northern Minnesota (USA). Ecosystems.

Schulte, L.A., Mladenoff, D.J., in press. Wind and fire regimes in northern Wisconsin (USA) forests: historic variability at the regional scale. Ecology.

Seiler, W., Crutzen, P.J., 1980. Estimates of gross and net fluxes of carbon between the biosphere and the atmosphere from biomass burning. Climate Change 2, 207–247.

Smith, M.L., Martin, M.E., 2001. A plot-based method for rapid estimation of forest canopy chemistry. Can. J. For. Res. 31, 549–555.

Smithwick, E.A.H., Harmon, M.E., Remillard, S.M., Acker, S.A., Franklin, J.F., 2002. Potential upper bounds of carbon stores in forests of the Pacific Northwest. Ecol. Appl. 12, 1303–1307.

Sprugel, D.G., 1984. Density, biomass, productivity, and nutrient-cycling changes during stand developments in wave-regenerated balsam fir forests. Ecol. Monogr. 54, 165–186.

Stone, J.N., MacKinnon, A., Parminter, J.V., Lertzman, K.P., 1998. Coarse woody debris decomposition documented over 65 years on southern Vancouver Island. Can. J. For. Res. 28, 788–793.

Swetnam, T.W., 1993. Fire history and climate change in Giant Sequoia groves. Science 262, 885–889.

Tinker, D.B., Knight, D.H., 2000. Coarse woody debris following fire and logging in Wyoming lodge pole pine forests. Ecosystems 3, 472–483.

Turner, M.G., Romme, W.H., 1994. Landscape dynamics in crown fire ecosystems. Landscape Ecol. 9, 59–77.

Tyrrell, L.E., Crow, T.R., 1994. Dynamics of dead wood in old-growth hemlock-hardwood forests of northern Wisconsin and northern Michigan. Can. J. For. Res. 24, 1672–1683.

Wallin, K.F., Raffa, K.F., 1998. Association of within-tree jack pine budworm feeding patterns with canopy level and within-needle variation of water, nutrient, and monoterpene concentrations. Can. J. For. Res. 28, 228–233.

Webb, S.L., 1989. Contrasting windstorm consequences in two forests, Itasca State Park, Minnesota. Ecology 70, 1167–1180.

Webb, S.L., Scanga, S.E., 2001. Windstorm disturbance without patch dynamics: twelve years of change in a Minnesota forest. Ecology 82, 893–897.

Weisberg, P.J., Swanson, F.J., 2003. Regional synchronicity in fire regimes of the western Cascades, USA. For. Ecol. Manage. 172, 17–28.

Zed, X., 1995. Hi-Rez Data Climatological Series. ZedX, Boalsburg, PA, USA.

Zhang, Q., Pregitzer, K.S., Reed, D.D., 1999. Catastrophic disturbance in the presettlement forests of the Upper Peninsula of Michigan. Can. J. For. Res. 29, 106–114.